REPORT DOCUMENTATION PAGE

Form Approved OMB NO. 0704-0188

1. REPORT DATE (DD-MM-YYYY)	2. REPORT TYPE	3. DATES COVERED (From - To)
	New Reprint	-

4. TITLE AND SUBTITLE
Biotemplated Synthesis of PZT Nanowires

5a. CONTRACT NUMBER
W911NF-11-1-0397

5b. GRANT NUMBER

5c. PROGRAM ELEMENT NUMBER
611102

6. AUTHORS
Kellye Cung, Booyeon J. Han, Thanh D. Nguyen, Sheng Mao, Yao-Wen Yeh, Shiyou Xu, Rajesh R. Naik, Gerald Poirier, Nan Yao, Prashant K. Purohit, Michael C. McAlpine

5d. PROJECT NUMBER

5e. TASK NUMBER

5f. WORK UNIT NUMBER

7. PERFORMING ORGANIZATION NAMES AND ADDRESSES
Princeton University
PO Box 36
87 Prospect Avenue
Princeton, NJ 08544 -2020

8. PERFORMING ORGANIZATION REPORT NUMBER

9. SPONSORING/MONITORING AGENCY NAME(S) AND ADDRESS (ES)
U.S. Army Research Office
P.O. Box 12211
Research Triangle Park, NC 27709-2211

10. SPONSOR/MONITOR'S ACRONYM(S)
ARO

11. SPONSOR/MONITOR'S REPORT NUMBER(S)
60738-EG.6

12. DISTRIBUTION AVAILIBILITY STATEMENT
Approved for public release; distribution is unlimited.

13. SUPPLEMENTARY NOTES
The views, opinions and/or findings contained in this report are those of the author(s) and should not contrued as an official Department of the Army position, policy or decision, unless so designated by other documentation.

14. ABSTRACT
Piezoelectric nanowires are an important class of smart materials for next-generation applications including energy harvesting, robotic actuation, and bioMEMS. Lead zirconate titanate (PZT), in particular, has attracted significant attention, owing to its superior electromechanical conversion performance. Yet, the ability to synthesize crystalline PZT nanowires with reproducible and well-controlled properties remains a challenge. Applications of common nanosynthesis methods to PZT are hampered by issues such as slow kinetics, lack of suitable catalysts, and harsh reaction conditions. Here we report on a versatile biomimetic method, in which biotemplates are used to define PZT

15. SUBJECT TERMS
Biotemplated nanomaterials, piezoelectric nanowires, biomimetic synthesis, biomechanical energy harvesting

16. SECURITY CLASSIFICATION OF:			17. LIMITATION OF ABSTRACT	15. NUMBER OF PAGES	19a. NAME OF RESPONSIBLE PERSON
a. REPORT	b. ABSTRACT	c. THIS PAGE			Michael McAlpine
UU	UU	UU	UU		19b. TELEPHONE NUMBER 609-258-8613

Report Title

Biotemplated Synthesis of PZT Nanowires

ABSTRACT

Piezoelectric nanowires are an important class of smart materials for next-generation applications including energy harvesting, robotic actuation, and bioMEMS. Lead zirconate titanate (PZT), in particular, has attracted significant attention, owing to its superior electromechanical conversion performance. Yet, the ability to synthesize crystalline PZT nanowires with reproducible and well-controlled properties remains a challenge. Applications of common nanosynthesis methods to PZT are hampered by issues such as slow kinetics, lack of suitable catalysts, and harsh reaction conditions. Here we report on a versatile biomimetic method, in which biotemplates are used to define PZT nanostructures, allowing for rational control over composition and crystallographic orientation. Specifically, stoichiometric PZT nanowires were synthesized using both polysaccharide (alginate) and bacteriophage templates. The wires possessed measured piezoelectric constants of up to 132 pm/V after poling, among the highest reported for PZT nanomaterials. Further, integrated devices can generate up to 84 nWatt of power. These results suggest that biotemplated piezoelectric nanowires are attractive candidates for ultrasensitive nanosensors, nanoactuators, and nanoscale energy harvesters.

REPORT DOCUMENTATION PAGE (SF298)
(Continuation Sheet)

Continuation for Block 13

ARO Report Number 60738.6-EG
Biotemplated Synthesis of PZT Nanowires ...

Block 13: Supplementary Note

Approved for public release; distribution is unlimited.

NANO LETTERS

Letter

pubs.acs.org/NanoLett

Biotemplated Synthesis of PZT Nanowires

Kellye Cung,[†] Booyeon J. Han,[‡] Thanh D. Nguyen,[§] Sheng Mao,[∥] Yao-Wen Yeh,[⊥] Shiyou Xu,[⊥] Rajesh R. Naik,[#] Gerald Poirier,[⊥] Nan Yao,[⊥] Prashant K. Purohit,[∥] and Michael C. McAlpine*[,§]

[†]Department of Chemical and Biological Engineering, Princeton University, Princeton, New Jersey 08544, United States

[‡]Department of Chemistry, Princeton University, Princeton, New Jersey 08544, United States

[§]Department of Mechanical and Aerospace Engineering, Princeton University, Princeton, New Jersey 08544, United States

[∥]Department of Mechanical Engineering and Applied Mechanics, University of Pennsylvania, Philadelphia, Pennsylvania 19104, United States

[⊥]Princeton Institute for Science and Technology of Materials, Princeton University, Princeton, New Jersey 08544, United States

[#]Materials & Manufacturing Directorate, Air Force Research Laboratory, Wright-Patterson Air Force Base, Wright-Patterson AFB, Ohio 45433, United States

S *Supporting Information*

ABSTRACT: Piezoelectric nanowires are an important class of smart materials for next-generation applications including energy harvesting, robotic actuation, and bioMEMS. Lead zirconate titanate (PZT), in particular, has attracted significant attention, owing to its superior electromechanical conversion performance. Yet, the ability to synthesize crystalline PZT nanowires with well-controlled properties remains a challenge. Applications of common nanosynthesis methods to PZT are hampered by issues such as slow kinetics, lack of suitable catalysts, and harsh reaction conditions. Here we report a versatile biomimetic method, in which biotemplates are used to define PZT nanostructures, allowing for rational control over composition and crystallinity. Specifically, stoichiometric PZT nanowires were synthesized using both polysaccharide (alginate) and bacteriophage templates. The wires possessed measured piezoelectric constants of up to 132 pm/V after poling, among the highest reported for PZT nanomaterials. Further, integrated devices can generate up to 0.820 μW/cm^2 of power. These results suggest that biotemplated piezoelectric nanowires are attractive candidates for stimuli-responsive nanosensors, adaptive nanoactuators, and nanoscale energy harvesters.

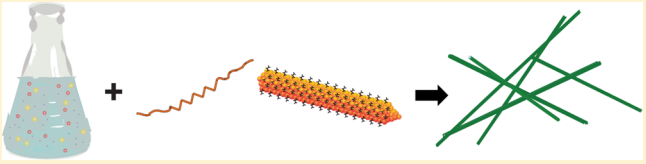

KEYWORDS: *Biotemplated nanomaterials, piezoelectric nanowires, biomimetic synthesis, biomechanical energy harvesting*

Piezoelectrics are a fascinating class of smart materials whose properties have been extensively characterized in the bulk, but much about their behavior at molecular dimensions is not well understood due to difficulties in synthesizing these materials at nanometer scales. Lead zirconate titanate, $Pb[Zr_xTi_{1-x}]O_3$ (PZT), possesses superior electromechanical properties, owing to its large piezoelectric charge constant,[1] rendering it particularly attractive for applications in biointerfaced mechanical probes,[2] bioMEMS devices,[3] nanorobotic actuators,[4] and energy harvesting.[5−7] One-dimensional piezoelectric nanostructures possess anisotropic geometries which may be more sensitive to unique deformation modes.[8,9] Furthermore, such nanostructures may be more resistant to fatigue and fracture than bulk films, potentially allowing nanowire-based piezoelectric devices to exhibit longer mechanical lifetimes and improved robustness.[10,11] Yet, the performance of PZT depends critically on its composition, and common methods for nanowire synthesis are poorly suited for stoichiometrically complex PZT.[12,13] For example, the vapor−liquid−solid (VLS) growth method is likely precluded due to the lack of suitable catalysts, and hydrothermal methods are encumbered by slow kinetics and the need for autoclaves.

Alternative routes are desired for the rational synthesis of PZT nanowires with well-controlled properties. Recently, a variety of biomimetic approaches have been developed which have enabled the biotemplating of a broad variety of materials with high crystallographic orientation and compositional and geometric control.[14−19] A wide range of biomolecules, including bone protein,[20] enzymes,[21] and DNA,[22] have been used to template the growth of nanostructures of functional materials, ranging from metals[23,24] to semiconductors[25,26] to superconductors.[27,28] These approaches offer several advantages over conventional synthetic methods, including milder reaction conditions,[19] greater size-control of nanocrystals,[24] and inherent structural and chemical specificity.[29] Indeed, many organisms have evolved the ability to nucleate and assemble materials of specified shape, size, and composition.[30,31] Not only does nature offer renewable and diverse resources with nanoscale dimensions, but many biomolecules have highly specific molecular recognition capabilities.[32−34] Some biotem-

Received: September 24, 2013
Revised: November 20, 2013
Published: November 25, 2013

dx.doi.org/10.1021/nl4035708 | *Nano Lett.* 2013, 13, 6197−6202

plates can even discriminate not only between different chemical species but also between different crystallographic phases of the same compound.[35−38]

Such biomolecules have not yet been used for the biotemplated synthesis of PZT nanomaterials, despite the prominence of this material in the ferroelectric and piezoelectric classes. Using such molecules to template the growth of PZT nanomaterials would not only provide a unique level of control over the properties of the resulting structures, it would also permit milder reaction conditions and fewer toxic byproducts. Such a development would allow for the reproducible and rational synthesis of nanowires with precise spatial, chemical, and crystallographic control, which could lead to an optimization of their fundamental properties and performance metrics as building blocks for next generation NEMS devices. Here, we present such an approach which involves only two components: (1) a PZT sol and (2) a suitable biotemplate. We also show that the resulting nanowires exhibit piezoelectric constants comparable to or better than previously reported values and that resulting integrated nanogenerators have high scaled power outputs.

Our approach proceeded as follows. First, the sol−gel approach is commonly used in the synthesis of crystalline thin films of stoichiometric PZT, in which a colloidal solution of the metal particles may be cast into a desired shape.[39] As a result, a sol route was determined to be the most readily adaptable for a variety of templates. As piezoelectric properties of PZT peak at the morphotropic phase boundary at $x = 0.53$,[40,41] this particular stoichiometry was chosen as a target for the biotemplate experiments. Figure 1a schematically outlines our

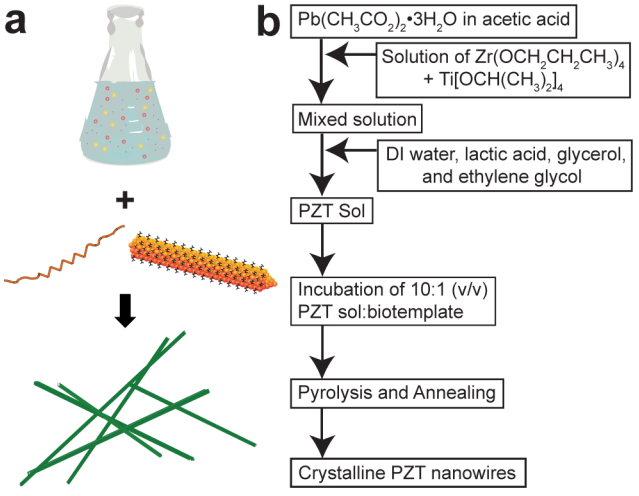

Figure 1. (a) Schematic of nanowire synthesis from a sol and appropriate biotemplates. (b) Flowchart illustrating the procedure for synthesis of biotemplated PZT nanowires.

approach. First, a $Pb(Zr_{0.53}Ti_{0.47})O_3$ sol was prepared from lead acetate, zirconium *n*-propoxide, and titanium-isopropoxide (Figure 1b).[42] Stoichiometry was confirmed using EDX, and the sol was incubated with a biotemplate before undergoing heat treatments to form crystalline nanowires.

The anionic polysaccharide biopolymer alginate was chosen for the initial templating experiments. Alginate has been previously shown to preferentially bind and sequester divalent metal cations, thereby constraining their growth along the crystallographic axis during thermal transformations.[43,44] In what has been called the "egg-box" model, the polysaccharide chains of alginate are cross-linked by divalent metal cations (such as Ca^{2+}), which are effectively encapsulated within the polymer network in a spatially discrete fashion (Figure 2a).[43]

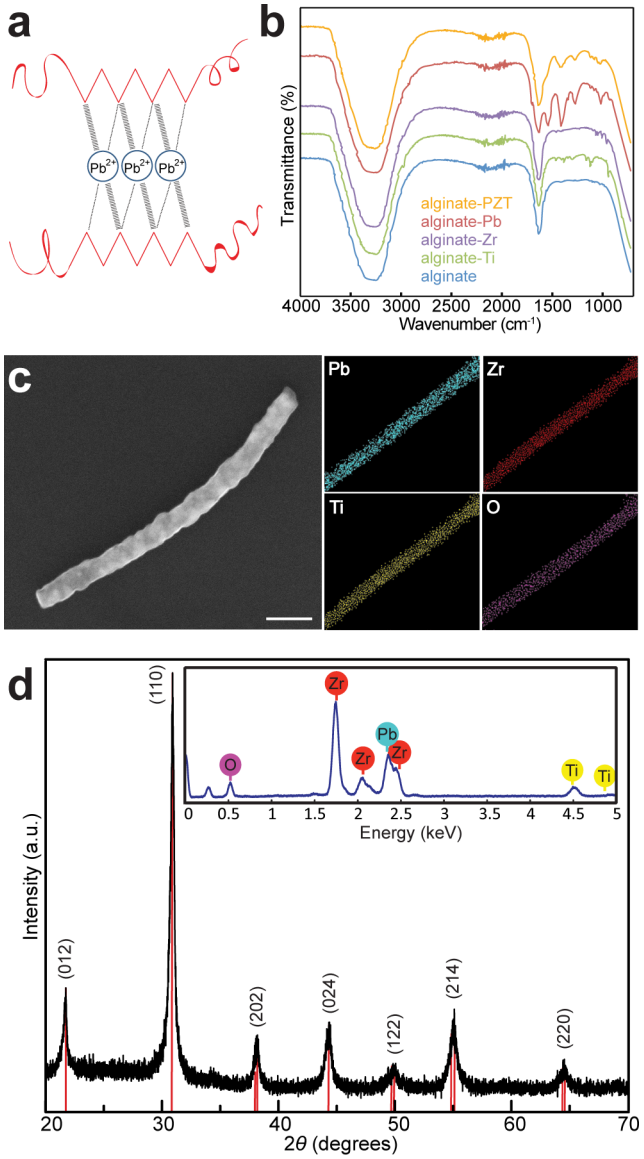

Figure 2. Alginate-templated PZT nanowires. (a) Schematic of preorganization of Pb^{2+} cations between alginate strands. (b) IR spectra corroborating association of alginate with Pb^{2+} cations. (c) SEM image of annealed nanowire, with corresponding EDX maps. Scale bar, 250 nm. (d) XRD spectrum of annealed nanowires, with the ICDD database data in red. Inset: EDX spectrum.

Upon thermal treatment, the polysaccharide network disappears, leaving behind only the nonorganic material in a preformed fiber shape. A 1:10 ratio of template-to-sol was found to yield the greatest quantity of high quality nanowires. Samples were pyrolized at 450 °C to carbonize the template and annealed at 725 °C to yield the desired perovskite phase. For both heating steps, a ramp rate of 1 °C/min was found to be optimal for wire formation, as faster rates led to template degradation and resulted in only discrete nanoparticles.

A series of control experiments was carried out to confirm that it was in fact the biopolymers that were responsible for the formation of the wire structures. No wire structures were

dx.doi.org/10.1021/nl4035708 | *Nano Lett.* 2013, 13, 6197−6202

observed if alginate was omitted, if there was insufficient incubation of template and sol, or if a TiO_2 sol was used instead. Additionally, infrared spectroscopy (IR) experiments were performed to determine whether it was the Pb^{2+} cation that associates with alginate. When alginate was incubated with individual Pb, Zr, and Ti precursors, IR spectra (Figure 2b) showed that the Pb-only sample most closely resembled that of the PZT spectrum, while the Zr and Ti spectra were markedly different. Both the Pb-alginate and PZT-alginate spectra exhibited peaks occurring near 1020 cm^{-1} and 1270 cm^{-1}, which have previously been reported as indicators of lead association.[45] A qualitative EDX elemental color heat map (Figure 2c) of the nanowires demonstrated that the elements were uniformly distributed over the entire length. X-ray diffraction (XRD) further corroborated EDX data (Figure 2d) and matched the ICDD database spectrum for perovskite $Pb(Zr_{0.53}Ti_{0.47})O_3$.

Next, we investigated whether this same experimental protocol would be successful with other biotemplates. M13 bacteriophage was chosen as a second template because (1) it possesses an inherently thin wiry structure (1 μm in length, 20 nm in width),[46] (2) it can be easily reproduced in great quantities via bacterial infection, and (3) it can be customized to bind compounds of interest with tailorable specificities based on the phage display process.[14] M13 is a virus that is encapsulated by thousands of coat proteins, to which functional motifs can be fused.[47,48] These fusion sequences are simultaneously linked with the native genetic material of the virus, allowing for exact copies to be easily reproduced in high quantities by bacterial infection. The fusion peptides are displayed at high densities with well-defined spacings on the nanometer scale, because the capsid proteins have a homogeneous size-distribution.[49] Phage-displayed peptides thus serve as robust and versatile templates with programmable genetic control over composition and phase of nanomaterials. Interestingly, the native phage have recently been found to exhibit piezoelectricity when terminated with glutamate groups, although with small coupling coefficients (d_{33} < 8 pm/V).[50]

As negatively charged carboxyl groups can bind cations,[51] M13 phages were genetically engineered to display glutamate groups all along their surface. Specifically, the triglutamate sequence, EEE, was fused to each of the 2700 copies of the pVIII coat protein of the virion, creating a high density display of the functional motif (Figure 3a). It was found that the heat treatment and template−sol ratio used for alginate were equally optimal for the phage biotemplate. By contrast, when a random phage library was utilized, no nanowires were observed (see Supporting Information). Selected area electron diffraction (SAED, see Supporting Information) revealed that the wires were amorphous prior to annealing but became polycrystalline after the thermal treatment. Annealed nanowires were examined using scanning electron microscopy, and it was found that large numbers of wires of uniform morphology could be readily generated (Figure 3b) with small diameters of <50 nm (inset, Figure 3b). EDX analysis confirmed the desired stoichiometry of $Pb(Zr_{0.53}Ti_{0.47})O_3$ (see Supporting Information). High-resolution transmission electron microscopy (HRTEM) indicated that the wires have a lattice spacing of 4.1 Å (Figure 3c), which is expected from this composition and crystal form of PZT.[52]

To determine the fundamental performance properties of these biotemplated PZT nanowires, the piezoelectric coefficient, d_{33}, which represents the induced polarization per unit

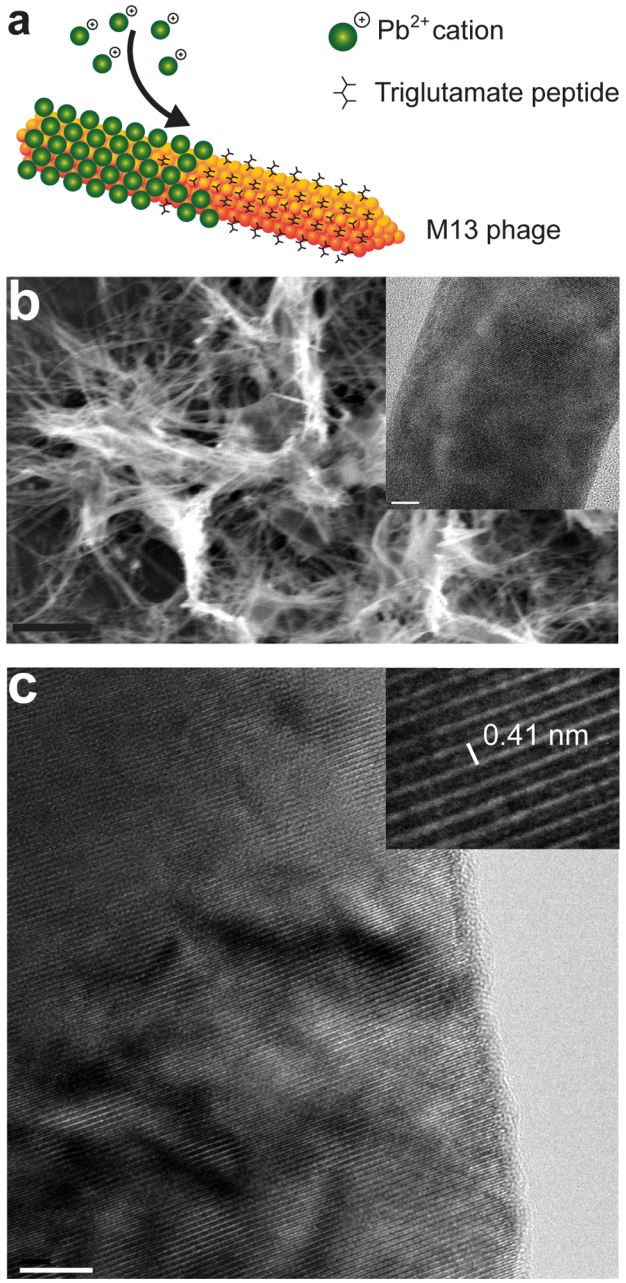

Figure 3. Phage-templated PZT nanowires. (a) Pb^{2+} cations bind to genetically engineered M13 bacteriophage displaying surface triglutamate (EEE) residues. (b) SEM image of annealed nanowires. Scale bar, 2 μm. Inset: HRTEM image of a single nanowire. Scale bar, 5 nm. (c) HRTEM image of a nanowire and inset demonstrating a lattice spacing of 0.41 nm. Scale bar, 5 nm.

stress applied in the poling direction, was measured using piezoresponse force microscopy (PFM). Here, an AC signal was applied between the AFM tip (NT-MDT, NSG03/Pt, 35 nm resolution) and a bottom contact electrode. A single wire was located and poled by applying 100 kV/cm to the AFM tip while scanning slowly in contact mode. Subsequently, d_{33} was determined by ramping the applied voltage from 0 to 10 V and measuring the piezoelectric displacement. Before poling, the average d_{33} measured at different points along the wire was 21 ± 2.3 pm/V, which subsequently increased to 132 ± 8.4 pm/V after poling (Figure 4a). This is on par with or larger than the values found for microfabricated PZT ribbons.[53−55]

dx.doi.org/10.1021/nl4035708 | Nano Lett. 2013, 13, 6197−6202

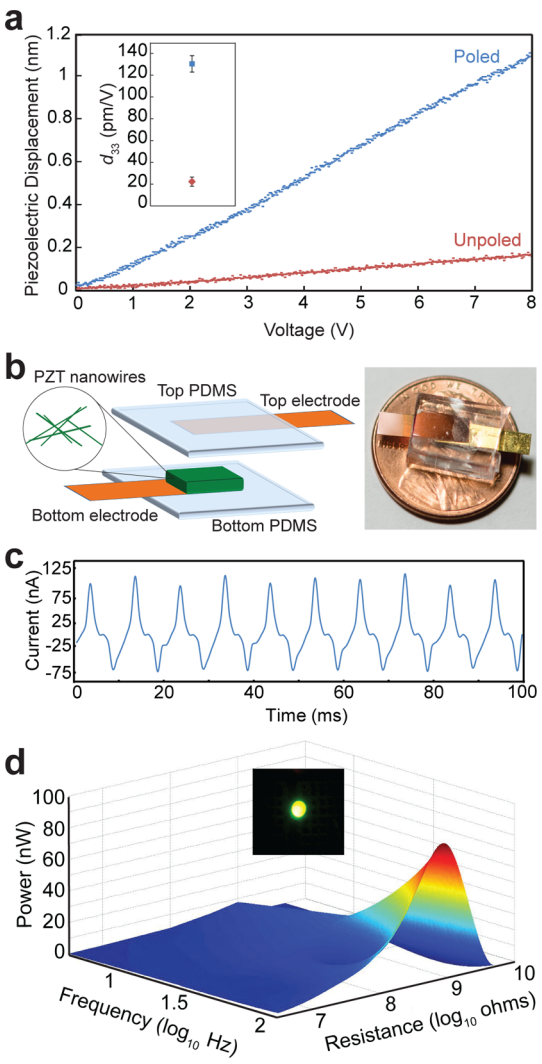

Figure 4. Characterization of piezoelectric properties of phage-templated nanowires. (a) Piezoresponse amplitude of a single wire, before and after poling. Inset: average d_{33} measured over the length of the wire, and standard deviation with N = 5 locations. (b) Construction of a device composed of biotemplate synthesized nanowires and a photo of the completed device. (c) Short-circuit current signal generated while applying a force on the device at 100 Hz. (d) Power output of the device as a function of both the frequency of the applied force and the magnitude of the external resistive load. Inset: photo of an LED illuminated by stored power generated by the device.

Next, as a proof-of-concept for energy harvesting applications, multiwire devices were fabricated from assembled films of biotemplated PZT nanowires. A collection of wires was sandwiched between gold-coated electrodes and encapsulated in PDMS (Figure 4b). To measure the power output of the device, compressive forces were applied periodically using a vibration generator connected to a mechanical indenter. Measurements were conducted at various resistive loads and frequencies while recording current signals (Figure 4c). Power was calculated via I^2R and found to peak at a value of 84 nW at a frequency of 100 Hz and a matching load of 1 GΩ (Figure 4d), which closely matched the internal resistance of the device itself. For a 3.2 mm × 3.2 mm × 170 μm film, this translates to normalized powers of 0.820 μW/cm^2 or 48.3 μW/cm^3. These values are appreciably greater than previously cited values of 0.03 μW for nanofibers[56] and 0.2 μW/cm^2[57] and 11 μW/cm^3 for thin films.[58] Lastly, the device was used to power a light-emitting diode (LED). A circuit was built with a rectifying bridge and a 25 μF capacitor. After actuating the device at 25 Hz for 20 min, sufficient power was generated to illuminate a commercial LED for ∼1 s (Figure 4d).

Finally, a one-dimensional model for the system was developed to corroborate the experimental results (details in the Supporting Information). This model estimates the power as

$$P = \frac{A^2}{\varphi_u^2}\frac{R}{(R+R_i)^2} \sim \frac{A^2 d_{33}^2 Y^2}{\varepsilon^2}\frac{R}{(R+R_i)^2}$$

where A is the amplitude of the time-varying deformation, R is the external resistive load, φ_u is an electromechanical conversion factor, equal to the ratio of the permittivity (ε) to the electromechanical coupling coefficient, Y is the Young's modulus, and R_i is intrinsic resistance. The PZT nanowire-based film is taken to have negligible capacitance and therefore be purely resistive. Intrinsic resistance was calculated to be ∼1 GΩ, which agrees with both the measured value, and consequently with the value at peak power output. Significantly, across various frequencies, all theoretical power calculations were found to be within 10% of experimental results (see Supporting Information).

In conclusion, crystalline PZT nanowires with excellent piezoresponses were synthesized via a biomimetic approach using a variety of biotemplates. The nanowires were found to have high crystallinity, well-controlled stoichiometries, and exhibit excellent d_{33} values. Further, nanogenerators comprised of collections of the wires were capable of generating 84 nW of power. In addition to being able to rationally tailor material properties with high precision, this method can also be adapted to template more complex architectures or different materials. For example, many biomolecules, including M13 phage, have been shown capable of forming nanorings and three-dimensional structures.[59] Future work will also look into increasing yield by further optimizing sol-template ratios, as well as methods for controlled assembly of these nanowires by transfer printing,[55] flow alignment,[60] Langmuir–Blodgett assembly,[61] dry transfer,[62] or dielectrophoresis approaches.[63] The ability to synthesize high-quality, high-performance piezoelectric nanowires and more sophisticated shapes using this novel, sustainable synthesis route could have profound implications for nanogenerators, soft robotics, self-powered nanosensors, and bioNEMS devices.

■ ASSOCIATED CONTENT

Supporting Information

Experimental details and supporting data. This material is available free of charge via the Internet at http://pubs.acs.org.

■ AUTHOR INFORMATION

Corresponding Author

*E-mail: mcm@princeton.edu.

Notes

The authors declare no competing financial interest.

■ ACKNOWLEDGMENTS

K.C. thanks Karthikeyan Rajendran for assistance with MATLAB and Lily Cheung and Nina Masters for assistance with figures. M.C.M. acknowledges support of this work by the

Army Research Office (No. W911NF-11-1-0397) and the Air Force Office of Scientific Research (No. FA9550-12-1-0367). P.K.P. acknowledges support by the Army Research Office (W-911NF-11-1-0494). N.Y. acknowledges the partial support of the National Science Foundation-MRSEC program through the Princeton Center for Complex Materials (DMR-0819860). R.R.N. acknowledges funding support from the Air Force Office of Scientific Research.

REFERENCES

(1) Guo, R.; Cross, L. E.; Park, S. E.; Noheda, B.; Cox, D. E.; Shirane, G. *Phys. Rev. Lett.* **2000**, *84*, 5423−5426.
(2) Nguyen, T. D.; Deshmukh, N.; Nagarah, J. M.; Kramer, T.; Purohit, P. K.; Berry, M. J.; McAlpine, M. C. *Nat. Nanotechnol.* **2012**, *7*, 587−593.
(3) Hong, K.-I.; Kim, S.-B.; Kim, S.-J.; Choi, D.-K. In Cantilever-type PZT microsensor using resonance frequency for bioMEMS application. *Proc. Int. Symp. Microelectron.*, 2001; International Society for Optics and Photonics: Bellingham, WA, 2001; pp 337−344.
(4) Choi, H.; Shin, D.; Ryuh, Y.; Han, C. In Development of a micro manipulator using a microgripper and PZT actuator for microscopic operations. *IEEE Int. Conf. Rob. Biomimetics*, 2011; IEEE: New York, 2011; pp 744−749.
(5) Wang, X.; Shi, J. Piezoelectric Nanogenerators for Self-powered Nanodevices. In *Piezoelectric Nanomaterials for Biomedical Applications*; Ciofani, G., Menciassi, A., Eds.; Springer: Berlin, 2012; pp 135−172.
(6) Tressler, J. F.; Alkoy, S.; Newnham, R. E. *J. Electroceram.* **1998**, *2*, 257−272.
(7) Xu, S.; Hansen, B. J.; Wang, Z. L. *Nat. Commun.* **2010**, *1*, 93.
(8) Bai, S.; Xu, Q.; Gu, L.; Ma, F.; Qin, Y.; Wang, Z. L. *Nano Energy* **2012**, *1*, 789.
(9) Platt, S. R.; Farritor, S.; Haider, H. *IEEE/ASME Trans. Mechatron* **2005**, *10*, 240−252.
(10) Wang, X. *Nano Energy* **2012**, *1*, 13−24.
(11) Kumar, B.; Kim, S.-W. *J. Mater. Chem.* **2011**, *21*, 18946−18958.
(12) Qi, Y.; Nguyen, T. D.; Purohit, P. K.; McAlpine, M. C. Stretchable Piezoelectric Nanoribbons for Biocompatible Energy Harvesting. In *Stretchable Electronics*; Someya, T., Ed.; Wiley-VCH: Weinheim, Germany, 2012; pp 111−139.
(13) Rørvik, P. M.; Grande, T.; Einarsrud, M.-A. *Adv. Mater.* **2011**, *23*, 4007−4034.
(14) Mao, C.; Solis, D. J.; Reiss, B. D.; Kottmann, S. T.; Sweeney, R. Y.; Hayhurst, A.; Georgiou, G.; Iverson, B.; Belcher, A. M. *Science* **2004**, *303*, 213−217.
(15) Hall, S. R. *Adv. Mater.* **2006**, *18*, 487−490.
(16) Yao, H.; Zheng, G.; Li, W.; McDowell, M. T.; Seh, Z. W.; Liu, N.; Lu, Z.; Cui, Y. *Nano Lett.* **2013**, *13*, 3385−3390.
(17) Dickerson, M. B.; Sandhage, K. H.; Naik, R. R. *Chem. Rev.* **2008**, *108*, 4935−4978.
(18) Mann, S.; Archibald, D. D.; Didymus, J. M.; Douglas, T.; Heywood, B. R.; Meldrum, F. C.; Reeves, N. J. *Science* **1993**, *261*, 1286−1292.
(19) Sarikaya, M.; Tamerler, C.; Jen, A. K.-Y.; Schulten, K.; Baneyx, F. *Nat. Mater.* **2003**, *2*, 577−585.
(20) Ogasawara, W.; Shenton, W.; Davis, S. A.; Mann, S. *Chem. Mater.* **2000**, *12*, 2835−2837.
(21) Kisailus, D.; Truong, Q.; Amemiya, Y.; Weaver, J. C.; Morse, D. E. *Proc. Natl. Acad. Sci.* **2006**, *103*, 5652−5657.
(22) Weizmann, Y.; Patolsky, F.; Popov, I.; Willner, I. *Nano Lett.* **2004**, *4*, 787−792.
(23) Wnęk, M.; Górzny, M. Ł.; Ward, M. B.; Wälti, C.; Davies, A. G.; Brydson, R.; Evans, S. D.; Stockley, P. G. *Nanotechnology* **2013**, *24*, 025605.
(24) Vijayaraghavan, K.; Nalini, S. P. *Biotechnol. J.* **2010**, *5*, 1098−1110.
(25) Sierra-Sastre, Y.; Dayeh, S. A.; Picraux, S. T.; Batt, C. A. *ACS Nano* **2010**, *4*, 1209−17.
(26) Nithyaja, B.; Vishnu, K.; Mathew, S.; Radhakrishnan, P.; Nampoori, V. P. N. *J. Appl. Phys.* **2012**, *112*, 064704.
(27) Boston, R.; Carrington, A.; Walsh, D.; Hall, S. R. *CrystEngComm* **2013**, *15*, 3763−3766.
(28) Hall, S. R.; Hall, C. F.; Hansberry, K.; Wimbush, S. C.; Shida, Y.; Ogasawara, W. *Supercond. Sci. Technol.* **2012**, *25*, 035009.
(29) Estroff, L. A. *Chem. Rev.* **2008**, *108*, 4329−4331.
(30) Faramarzi, M. A.; Sadighi, A. *Adv. Colloid Interface Sci.* **2013**, *189*−*190*, 1−20.
(31) Yamashita, I. *J. Mater. Chem.* **2008**, *18*, 3813−3820.
(32) Katz, E.; Willner, I. *Angew. Chem., Int. Ed.* **2004**, *43*, 6042−6108.
(33) Huang, Y.; Chiang, C.-Y.; Lee, S. K.; Gao, Y.; Hu, E. L.; Yoreo, J. D.; Belcher, A. M. *Nano Lett.* **2005**, *5*, 1429−1434.
(34) Tomczak, M. M.; Gupta, M. K.; Drummy, L. F.; Rozenzhak, S. M.; Naik, R. R. *Acta Biomater.* **2009**, *5*, 876−882.
(35) Galloway, J. M.; Bramble, J. P.; Staniland, S. S. *Chemistry* **2013**, *19*, 8710−25.
(36) Galloway, J. M.; Bird, S. M.; Bramble, J. P.; Critchley, K.; Staniland, S. S. *Mater. Res. Soc. Symp. Proc.* **2013**, 1569.
(37) Canabady-Rochelle, L. L.; Belton, D. J.; Deschaume, O.; Currie, H. A.; Kaplan, D. L.; Perry, C. C. *Biomacromolecules* **2012**, *13*, 683−90.
(38) Bai, J.; Zhong, X.; Jiang, S.; Huang, Y.; Duan, X. *Nat. Nanotechnol.* **2010**, *5*, 190−194.
(39) Schwartz, R. W.; Boyle, T. J.; Lockwood, S. J.; Sinclair, M. B.; Dimos, D.; Buchheit, C. D. *Integr. Ferroelectr.* **1995**, *7*, 259−277.
(40) Carim, A. H.; Tuttle, B. A.; Doughty, D. H.; Martinez, S. L. *J. Am. Ceram. Soc.* **1991**, *74*, 1455−1458.
(41) Lucuţa, P. G.; Teodorescu, V.; Vasiliu, F. *Appl. Phys. A: Mater. Sci. Process.* **1985**, *37*, 237−242.
(42) Hsu, Y.-C.; Wu, C.-C.; Lee, C.-C.; Cao, G. Z.; Shen, I. Y. *Sens. Actuators, A* **2004**, *116*, 369−377.
(43) Sikorski, P.; Mo, F.; Skjåk-Bræk, G.; Stokke, B. T. *Biomacromolecules* **2007**, *8*, 2098−2103.
(44) Smidsrød, O. *Trends Biotechnol.* **1990**, *8*, 71−78.
(45) Papageorgiou, S. K.; Kouvelos, E. P.; Favvas, E. P.; Sapalidis, A. A.; Romanos, G. E.; Katsaros, F. K. *Carbohydr. Res.* **2010**, *345*, 469−473.
(46) Sidhu, S. S. *Biomol. Eng.* **2001**, *18*, 57−63.
(47) Merzlyak, A.; Lee, S.-W. *Bioconjugate Chem.* **2009**, *20*, 2300−2310.
(48) Flynn, C. E.; Lee, S.-W.; Peelle, B. R.; Belcher, A. M. *Acta Mater.* **2003**, *51*, 5867−5880.
(49) Lee, S. K.; Yun, D. S.; Belcher, A. M. *Biomacromolecules* **2006**, *7*, 14−7.
(50) Lee, B. Y.; Zhang, J.; Zueger, C.; Chung, W.-J.; Yoo, S. Y.; Wang, E.; Meyer, J.; Ramesh, R.; Lee, S.-W. *Nat. Nanotechnol.* **2012**, *7*, 351−356.
(51) Cannan, R. K.; Kibrick, A. *J. Am. Chem. Soc.* **1938**, *60*, 2314−2320.
(52) Kanno, I.; Kotera, H.; Wasa, K.; Matsunaga, T.; Kamada, T.; Takayama, R. *J. Appl. Phys.* **2003**, *93*, 4091−4096.
(53) Qi, Y.; Kim, J.; Nguyen, T. D.; Lisko, B.; Purohit, P. K.; McAlpine, M. C. *Nano Lett.* **2011**, *11*, 1331−1336.
(54) Nguyen, T. D.; Nagarah, J. M.; Qi, Y.; Nonnenmann, S. S.; Morozov, A. V.; Li, S.; Arnold, C. B.; McAlpine, M. C. *Nano Lett.* **2010**, *10*, 4595−4599.
(55) Qi, Y.; Jafferis, N. T.; Lyons, K., Jr; Lee, C. M.; Ahmad, H.; McAlpine, M. C. *Nano Lett.* **2010**, *10*, 524−528.
(56) Chen, X.; Xu, S.; Yao, N.; Shi, Y. *Nano Lett.* **2010**, *10*, 2133−2137.
(57) Xie, J.; Mane, X. P.; Green, C. W.; Mossi, K. M.; Leang, K. K. *J. Intell. Mater. Syst. Struct.* **2010**, *21*, 243−249.
(58) Liu, H.; Tay, C. J.; Quan, C.; Kobayashi, T.; Lee, C. *J. Microelectromech. Syst.* **2011**, *20*, 1131−1142.
(59) Nam, K. T.; Peelle, B. R.; Lee, S.-W.; Belcher, A. M. *Nano Lett.* **2004**, *4*, 23−27.
(60) Huang, Y.; Duan, X.; Wei, Q.; Lieber, C. M. *Science* **2001**, *291*, 630−633.
(61) Whang, D.; Jin, S.; Lieber, C. M. *Nano Lett.* **2003**, *3*, 951−954.

(62) Fan, Z.; Ho, J. C.; Jacobson, Z. A.; Razavi, H.; Javey, A. *Proc. Natl. Acad. Sci.* **2008**, *105*, 11066−11070.
(63) Freer, E. M.; Grachev, O.; Duan, X.; Martin, S.; Stumbo, D. P. *Nat. Nanotechnol.* **2010**, *5*, 525−530.